Electronic Supplementary Material (ESI) for Catalysis Science & Technology.

Supporting information

Variation of Redox Activity and Synergestic Effect for Improving Preferential Oxidation of CO in H_2-rich Gases in Porous Pt/CeO_2-Co_3O_4 Catalysts

Baocang Liu[a,b], Yongxin Liu[a], Heting Hou[a], Yang Liu[a], Qin Wang[a,b], Jun Zhang[a,b]*

[a]*College of Chemistry and Chemical Engineering, Inner Mongolia University, Hohhot 010021, P. R. China.* [b]*Inner Mongolia Key Lab of Nanoscience and Nanotechnology, Inner Mongolia University, Hohhot 010021, P. R. China Tel: 0086 471 4992175; Fax: 0086 471 4992278; Email:cejzhang@imu.edu.cn*

Table S1 The compositions of macro- and meso-porous Pt/CeO_2-Co_3O_4 catalysts estimated by ICP-MS and ICP-AES measurements.

Catalysts	Theoretical molar ratio of Co/Ce	Actual molar ratio of Co/Ce	Theoretical content Pt (wt.%)	Actual content Pt (wt.%)
Pt/CeO_2	0:1	0:1	3	1.75
	7:3	5.7:3	3	1.37
Pt/CeO_2-Co_3O_4	1:1	0.9:1	3	1.68
	1:4	1:4.4	3	1.64
Pt/Co_3O_4	1:0	1:0	3	2.07

Table S2 The BET property of macro- and meso-porous CeO_2–Co_3O_4 supports and macro- and meso-porous Pt/CeO_2–Co_3O_4 catalysts.

Supports and Catalysts	S_{BET}($m^2.g^{-1}$)	V_p($cm^3.g^{-1}$)	D_p(nm)
CeO_2	72	0.13	3.7
Pt/CeO_2	66	0.11	3.6
(7:3)CeO_2–Co_3O_4	62	0.18	3.6
Pt/(7:3)CeO_2–Co_3O_4	57	0.16	3.3
(1:1)CeO_2–Co_3O_4	58	0.19	3.2
Pt/(1:1)CeO_2–Co_3O_4	54	0.14	3.1
(1:4)CeO_2–Co_3O_4	51	0.24	3.2
Pt/(1:4)CeO_2–Co_3O_4	46	0.23	3.2
Co_3O_4	29	0.24	2.2
Pt/Co_3O_4	24	0.20	2.1

Table S3 The nominal and actual H_2 consumption of reduction peaks of macro- and meso-porous Pt/CeO_2-Co_3O_4 catalysts with different Ce/Co molar ratios.

Catalysts	Nominal H_2 consumption (μmol $\cdot g_{Cat.}^{-1}$)	Actual H_2 consumption (μmol $\cdot g_{Cat.}^{-1}$)
Pt/CeO_2	4.44	3.11
Pt/(7:3)CeO_2-Co_3O_4	3.51	4.11
Pt/(1:1)CeO_2-Co_3O_4	4.26	7.21
Pt/(1:4)CeO_2-Co_3O_4	4.21	10.4
Pt/Co_3O_4	5.31	102.1

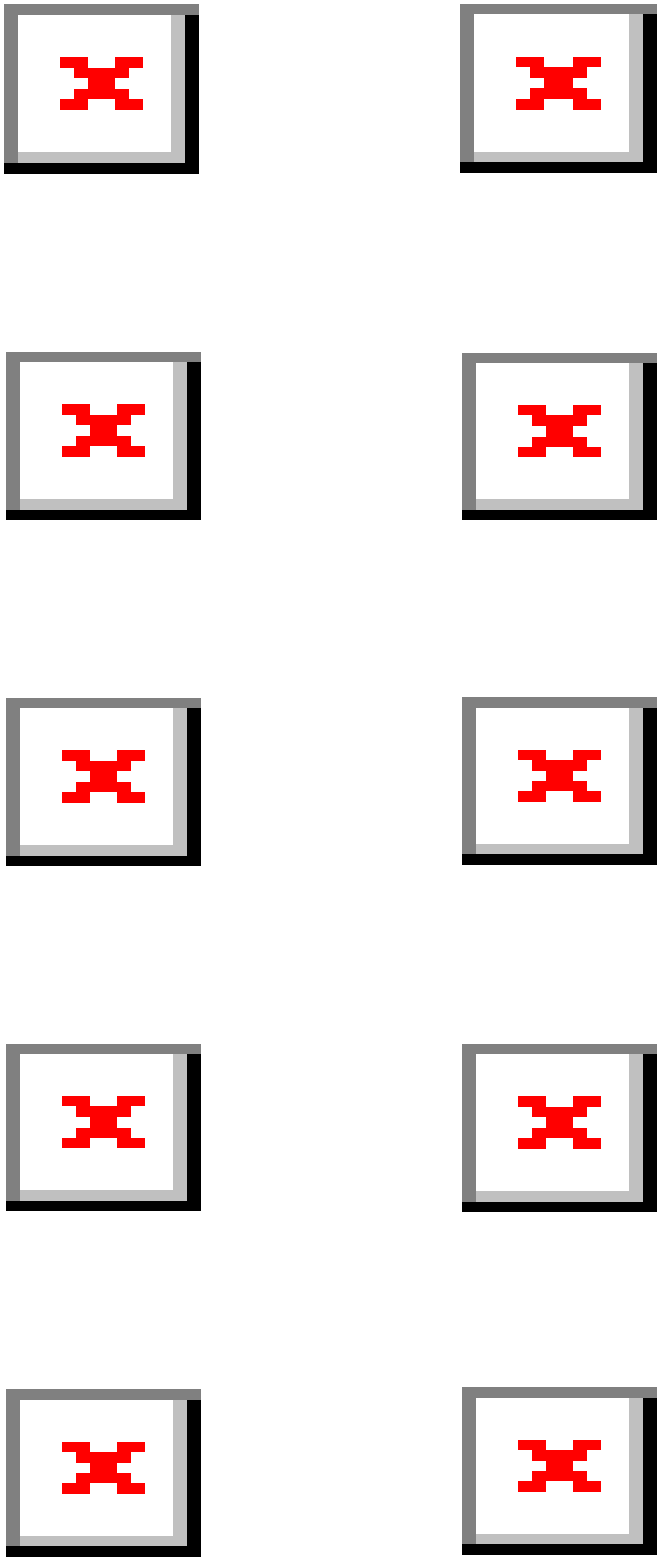

Fig.S1 SEM images of macro- and meso-porous CeO_2-Co_3O_4 supports with various molar ratios of Ce/Co at (a and b) 1:0, (c and d) 7:3, (e and f) 1:1, (g and h) 1:4, and (I and j) 0:1.

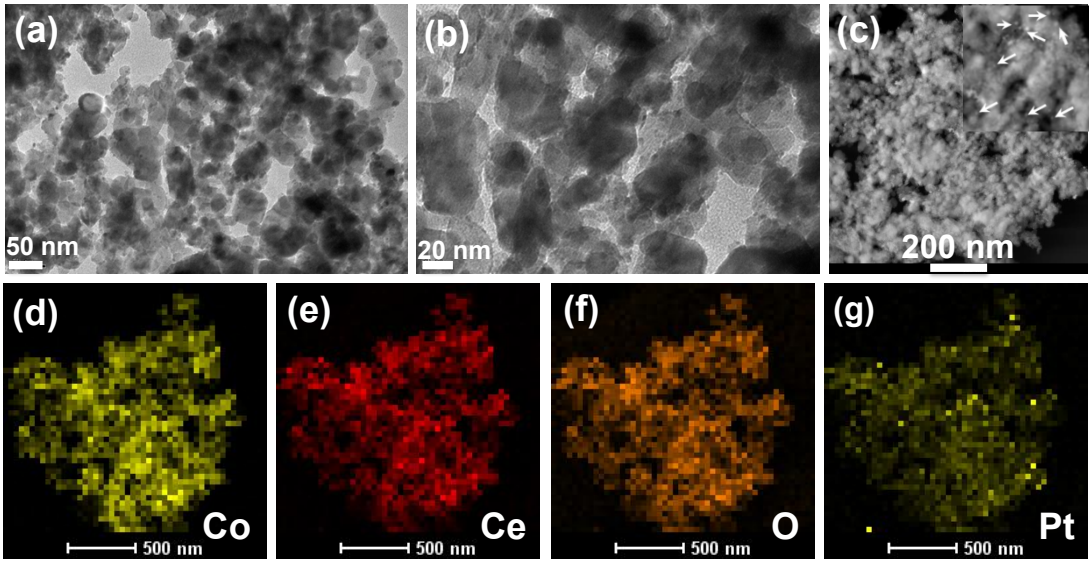

Fig. S2 (a and b) TEM images of powder Pt/(1:4) CeO_2-Co_3O_4 catalyst; the black spots indicated by arrows are Pt nanoparticles. (c) HAADF-STEM image of powder Pt/(1:4) CeO_2-Co_3O_4 catalyst; the light spots indicated by arrows are Pt nanoparticles. The inset image of (c) is the magnified STEM image of powder Pt/(1:4) CeO_2-Co_3O_4 catalyst. (d-g) EDX elemental mapping of Co, Ce, O, and Pt in powder Pt/(1:4)CeO_2-Co_3O_4 catalyst.

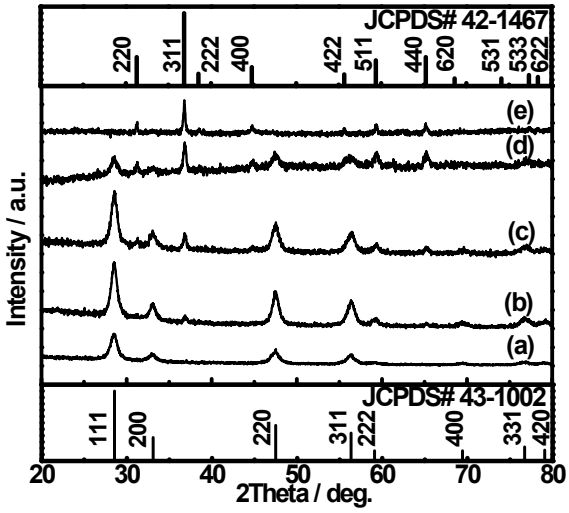

Fig.S3 XRD patterns of powder Pt/CeO_2–Co_3O_4 catalysts with various Ce/Co molar ratios at (a) 0:1, (b) 1:4, (c) 1:1, (d) 7:3, and (e) 1:0.

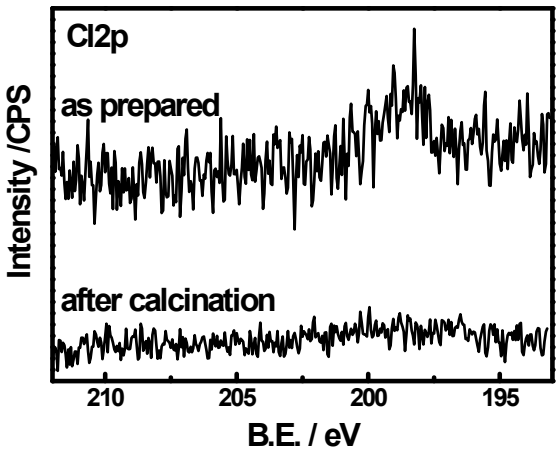

Fig.S4 XPS spectra of as prepared macro- and meso-porous Pt/(1:4)CeO_2-Co_3O_4 catalyst and macro- and meso-porous Pt/(1:4)CeO_2-Co_3O_4 catalyst after calcination at 450 °C.

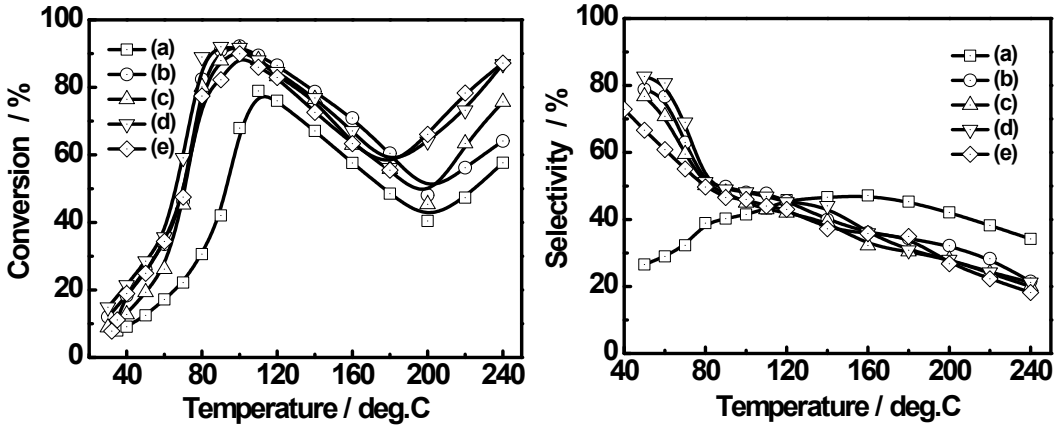

Fig.S5 CO conversion (left) and CO_2 selectivity (right) of CO PROX reaction in H_2-rich gases on powder (a) Pt/CeO_2, (b) Pt/(7:3)CeO_2–Co_3O_4, (c) Pt/(1:1)CeO_2-Co_3O_4, (d) Pt/(1:4)CeO_2–Co_3O_4, and (e) Pt/Co_3O_4 catalysts.

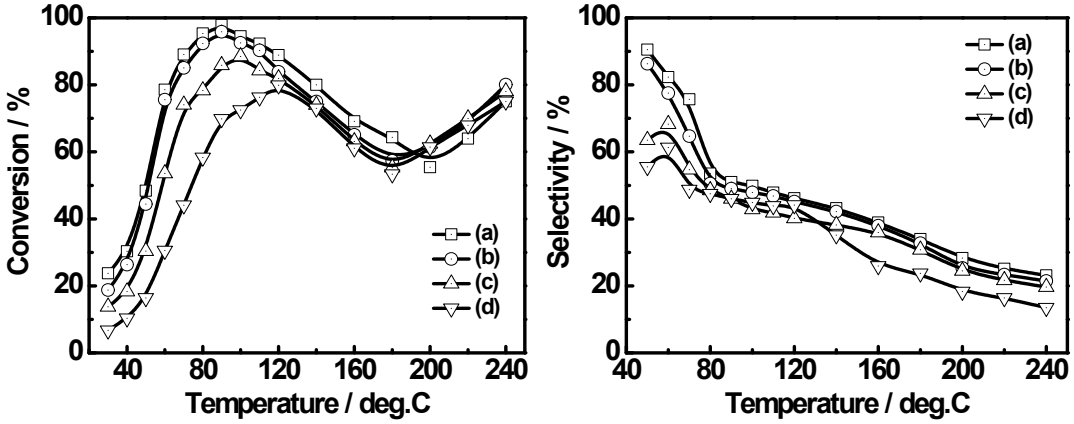

Fig.S6 CO conversion (left) and CO_2 selectivity (right) of CO PROX reaction in H_2-rich gases on macro- and meso-porous Pt/(1:4)CeO_2-Co_3O_4 performed under different space velocities at (a) 18,000, (b) 30,000, (c) 60,000, and (d) 90,000 $mL \cdot g^{-1} \cdot h^{-1}$.

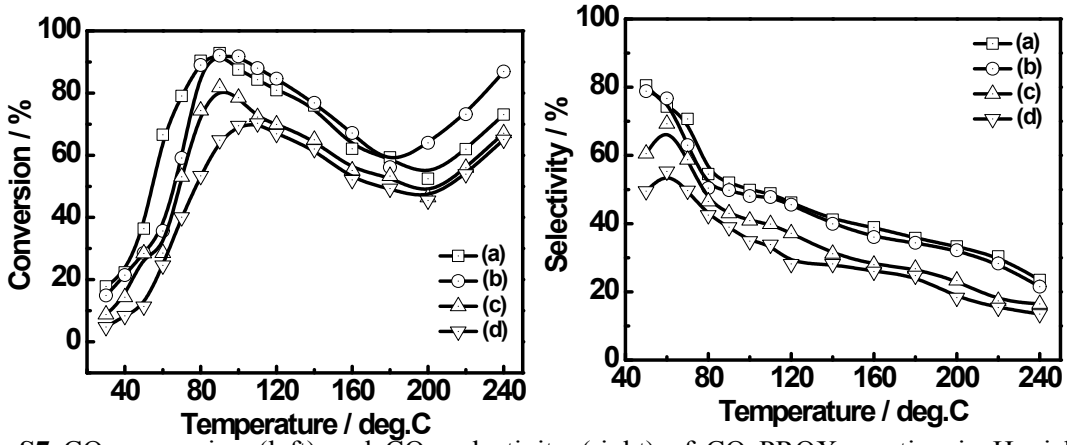

Fig.S7 CO conversion (left) and CO_2 selectivity (right) of CO PROX reaction in H_2-rich gases on powder Pt/(1:4)CeO_2-Co_3O_4 catalysts performed under different space velocities of (a) 18,000, (b) 30,000, (c) 60,000, and (d) 90,000 $mL \cdot g^{-1} \cdot h^{-1}$.